NRC·CNRC

NRC Publications Archive
Archives des publications du CNRC

Radical-initiated and thermally induced hydrogermylation of alkenes on the surfaces of germanium nanosheets

Yu, Haoyang; Helbich, Tobias; Scherf, Lavinia M.; Chen, Jian; Cui, Kai; Fässler, Thomas F.; Rieger, Bernhard; Veinot, Jonathan G. C.

This publication could be one of several versions: author's original, accepted manuscript or the publisher's version. / La version de cette publication peut être l'une des suivantes : la version prépublication de l'auteur, la version acceptée du manuscrit ou la version de l'éditeur.
For the publisher's version, please access the DOI link below./ Pour consulter la version de l'éditeur, utilisez le lien DOI ci-dessous.

Publisher's version / Version de l'éditeur:
https://doi.org/10.1021/acs.chemmater.7b04974
Chemistry of Materials, 2018-03-13

NRC Publications Record / Notice d'Archives des publications de CNRC:
https://nrc-publications.canada.ca/eng/view/object/?id=6dd4a654-fa49-404c-8648-8959a991b7ba
https://publications-cnrc.canada.ca/fra/voir/objet/?id=6dd4a654-fa49-404c-8648-8959a991b7ba

Access and use of this website and the material on it are subject to the Terms and Conditions set forth at https://nrc-publications.canada.ca/eng/copyright
READ THESE TERMS AND CONDITIONS CAREFULLY BEFORE USING THIS WEBSITE.

L'accès à ce site Web et l'utilisation de son contenu sont assujettis aux conditions présentées dans le site https://publications-cnrc.canada.ca/fra/droits
LISEZ CES CONDITIONS ATTENTIVEMENT AVANT D'UTILISER CE SITE WEB.

Questions? Contact the NRC Publications Archive team at PublicationsArchive-ArchivesPublications@nrc-cnrc.gc.ca. If you wish to email the authors directly, please see the first page of the publication for their contact information.

Vous avez des questions? Nous pouvons vous aider. Pour communiquer directement avec un auteur, consultez la première page de la revue dans laquelle son article a été publié afin de trouver ses coordonnées. Si vous n'arrivez pas à les repérer, communiquez avec nous à PublicationsArchive-ArchivesPublications@nrc-cnrc.gc.ca.

National Research Council Canada | Conseil national de recherches Canada

Canada

CHEMISTRY OF MATERIALS
Cite This: Chem. Mater. XXXX, XXX, XXX−XXX
Article
pubs.acs.org/cm

Radical-Initiated and Thermally Induced Hydrogermylation of Alkenes on the Surfaces of Germanium Nanosheets

Haoyang Yu,[†] Tobias Helbich,[‡] Lavinia M. Scherf,[§] Jian Chen,[∥] Kai Cui,[∥] Thomas F. Fässler,[§] Bernhard Rieger,[‡] and Jonathan G.C. Veinot*[,†]

[†]Department of Chemistry, University of Alberta, 11227 Saskatchewan Drive, Edmonton, Alberta T6G 2G2, Canada
[‡]Catalysis Research Center Wacker-Lehrstuhl für Makromolekulare Chemie, Department of Chemistry, Technische Universität München, Lichtenbergstraße 4, 85748 Garching, Germany
[§]Lehrstuhl für Anorganische Chemie mit Schwerpunkt Neue Materialien, Department of Chemistry, Technische Universität München, Lichtenbergstraße 4, 85748 Garching, Germany
[∥]Nanotechnology Research Centre, National Research Council Canada, 11421 Saskatchewan Drive, Edmonton, Alberta T6G 2M9, Canada

Supporting Information

ABSTRACT: The synthesis of germanium nanomaterials with well-defined surface chemistry is of considerable interest because of not only general scientific curiosity but also their vast potential in optoelectronics, energy storage, and the semiconductor industry. Herein, we report a straightforward preparative route that yields hydride-terminated germanium nanosheet (H-GeNS) monolayers via sonochemical exfoliation of hydride-terminated germanane flakes (HGe-flakes) derived from crystalline $CaGe_2$. We subsequently show that these freestanding H-GeNSs are readily functionalized by radical-initiated and thermally induced hydrogermylation. Furthermore, we demonstrate that following functionalization the crystal structure of the GeNSs remains intact, and the introduction of organic moieties to the GeNS surfaces imparts improved thermal stability and solvent compatibility.

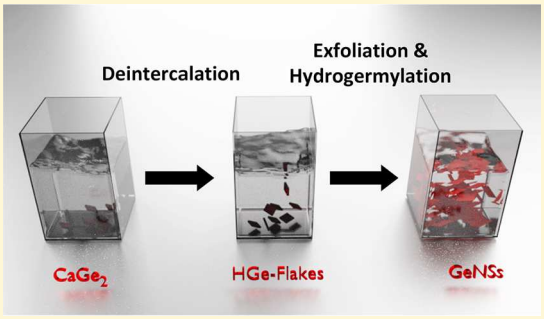

The preparation and applications of van der Waals materials has become an area of intense investigation because exfoliation of layered precursors can yield new materials with properties that differ substantially from their bulk material equivalents.[1−4] The prototypical van der Waals material is graphene; it exhibits tremendously high carrier mobility compared to graphite and is among the strongest materials known.[1,5,6] While the preparation and derivatization, as well as physical and chemical properties of graphene, are being studied widely, investigations of sheet materials of carbon's heavier periodic congeners (i.e., silicon and germanium) are far less prevalent.[2,7]

Doubtless, the limited number of studies of nanosheets of heavier group 14 elements is partly because there is no naturally occurring layered allotrope of silicon or germanium with a graphite-like structure. Epitaxially grown 2D elemental Si (silicene) and Ge (germanene) can only be achieved on metallic surfaces in ultrahigh vacuum condition,[8−10] and must be encapsulated to survive in ambient environment.[11] The search for a suitable layered precursor for Si sheets saw Wöhler deintercalate layered calcium disilicide ($CaSi_2$).[12] Stutzmann and co-workers extended this Ca-deintercalation methodology to prepare hydride-terminated germanane (or germanium nanosheets; GeNS) from layered calcium digermanide ($CaGe_2$).[13,14] Goldberger and co-workers revisited this approach, and mechanically exfoliated hydride-terminated Ge nanosheets (HGeNSs) as single- and few-layer sheets via Scotch Tape and polydimethylsiloxane lift-off.[7] HGeNSs prepared in this way possess a buckled honeycomb structure with surfaces crystallographically identical to Ge (111) oriented wafers.[9,15,16]

Exfoliated HGeNSs oxidize when exposed to ambient conditions—this behavior is similar to that of hydride-terminated Ge (111) wafer surfaces,[17−19] as well as germanene.[8,9] The introduction of covalently bonded layers onto the surfaces of GeNSs is of particular interest because of the expected chemical stability and solvent/medium compatibility they will impart. As well, modifying the molecular layer presents the opportunity to predictably tailor material properties (e.g., conductivity, processability, optical response, assembly, etc.).[19−27]

To date, only one solution route has been reported that affords functionalized GeNSs. Goldberger et al. prepared surface protected GeNSs by topotactically reacting layered

Received: November 29, 2017
Revised: March 12, 2018
Published: March 13, 2018

© XXXX American Chemical Society

DOI: 10.1021/acs.chemmater.7b04974
Chem. Mater. XXXX, XXX, XXX−XXX

$CaGe_2$ with small iodoalkanes (e.g., R-I; R = $—CH_3$, $—CH_2OCH_3$, $—CH_2CH═CH_2$, etc.).[28−30] While the materials produced by this approach exhibited improved ambient and thermal stability, the scope (i.e., length, reactivity, electronic properties, etc.) of the surface functionality is very limited; more importantly, it is not immediately clear how more complex surface functionalities could be introduced using this approach.

We, and others, have demonstrated various hydrosilylation protocols that afford convenient methods for modifying hydride-terminated silicon (111) surfaces,[19] silicon nanoparticles,[31−33] and silicane.[23,27] There have also been a few reports of hydrogermylation on Ge substrates and nanomaterials.[19−21] In this contribution, we report the first demonstration of radical-initiated and thermally induced hydrogermylation on HGeNSs, as well as detailed characterization of the resulting functionalized materials.

Calcium ions were topotactically deintercalated from crystalline $CaGe_2$ to afford hydride-terminated germanane flakes (HGe-flakes).[7] Exposure of $CaGe_2$ to cold (i.e., −30 °C) concentrated HCl for 1 week caused the characteristic flat gray appearance of $CaGe_2$ to become black with a shiny metallic luster (Scheme 1). A straightforward comparison of the

Scheme 1. Preparation of Hydride-Terminated Germanium Nanosheets: (i) −30 °C HCl for 1 Week, (ii) 3 h of Ultrasonication in Toluene

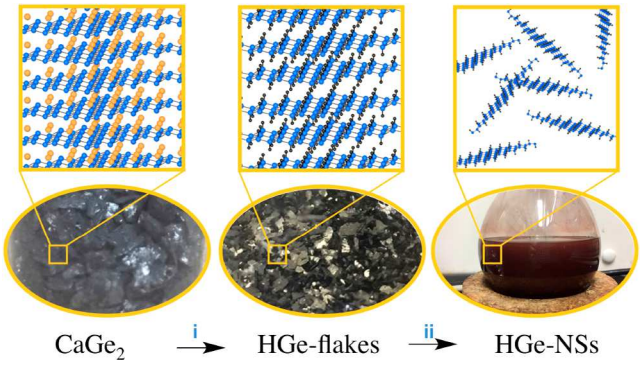

powder X-ray diffraction (XRD) pattern of $CaGe_2$ with that of the layered HGe-flakes provides insight into the deintercalation process (Figures S1 and S2). The diffraction pattern of the $CaGe_2$ is readily indexed to a tr6 unit cell while that of the HGe-flakes can be indexed to a hexagonal unit cell with a = 3.99 Å and c = 5.50 Å; these observations indicate the HGe-flakes are made up of stacked HGeNS. Surface hydride-termination was confirmed using FTIR spectroscopy, which shows a characteristic Ge−H feature at 2001 cm^{-1} (Figure 1a). Energy dispersive X-ray spectroscopy (EDX) of the HGe-flakes indicates the presence of germanium, as well as trace (i.e., <1 wt %) oxygen and Ca (Figure S3). Consistent with these results, the survey X-ray photoelectron spectrum indicates only Ca, Ge, O, and C are present at the sensitivity of the method (Figure S4). The high-resolution XP spectrum (Figure 1b) gives insight into the oxidation state of Ge atoms on the HGe-flake surface (i.e., within the top 10 nm)—deconvolution of the Ge 3d spectral region indicates 15 atom % Ge^{2+}.

HGeNSs were prepared via sonication of HGe-flakes in an appropriate organic solvent (e.g., toluene). This approach exploits the comparatively weak interlayer interactions (i.e., 72 meV per Ge atom) within HGe-flakes, which are dominated by

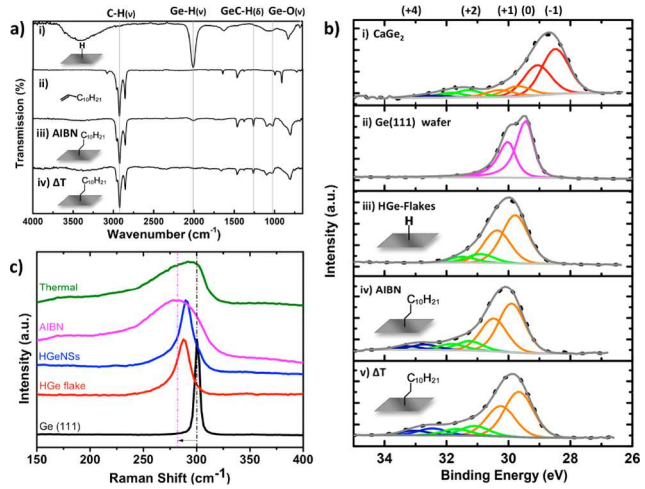

Figure 1. (a) Comparison of the FTIR spectra of indicated materials. (b) High-resolution XP spectra of the Ge 3d spectra region for the indicated materials. The deconvolution of each oxidation state has been fit to the Ge $3d_{5/2}$ and $3d_{3/2}$ spin−orbit pairs in the same color set. (c) Raman spectra of the indicated materials.

van der Waals forces and are of the same order of magnitude of interlayer bonding observed for graphite (i.e., 53.5 meV per C atom).[34,35] The degree of exfoliation impacts the physical appearance of the resulting HGeNSs.

After 5 min of ultrasonication the black HGe-flakes break up to yield a pink suspension; this suspension becomes deep red after an additional 55 min of treatment (i.e., 1 h of total sonication). Exfoliated HGeNSs agglomerate upon drying and readily oxidize as made evident by Ge−O associated features in the FTIR spectrum (not shown) hindering additional characterization; as a result surface functionalization was performed immediately following exfoliation.

Azobis(isobutyronitrile) (AIBN) radical-initiated hydrogermylation has previously been exploited for the derivatization of hydride-terminated germanium nanocrystals;[18] in this context, similar conditions were applied here to the functionalization of exfoliated HGeNSs. Based upon FTIR analysis, AIBN activated surface modification of HGeNSs with 1-dodecene in degassed toluene heated to 60 °C was completed after 12 h. At these temperatures no obvious surface modification was observed when the reaction mixture is heated in the absence of AIBN (i.e., there is no thermal activation of hydrogermylation). Consistent with alkyl derivatization, the FTIR spectrum (Figure 1a) of the dodecyl-functionalized NSs (i.e., dodecyl-GeNSs) shows the concomitant appearance of $\nu(C—H)_{asym}$ features at 2852 cm^{-1} and loss of ν(Ge—H) at 2001 cm^{-1} and ν(C═C) at 3078 cm^{-1}.[18] We also note that the ν(O—H) feature at 3400 cm^{-1} in the spectrum of HGe-flakes (Figure 1a) is substantially diminished in the spectrum of dodecyl-GeNSs (Figure 1a); we propose this observation arises because only the outer layers of the HGe-flakes are oxidized and because they are removed during purification due to their limited compatibility with nonpolar media.

Thermally induced hydrogermylation has also been demonstrated for Ge surfaces and nanosystems.[19,20,36] Here we extend this approach to the alkyl-termination of HGeNSs upon heating exfoliated HGe-flakes in neat 1-dodecene to 190 °C in an inert atmosphere. This procedure caused the initially deep red suspension to turn brown−gray after 2 h. The FTIR spectra of the recovered product are similar to those of functionalized

DOI: 10.1021/acs.chemmater.7b04974
Chem. Mater. XXXX, XXX, XXX−XXX

GeNSs prepared using radical-initiated reactions (Figure 1; *vide supra*).

Comparing the Raman spectra of crystalline Ge(111), HGe-flakes, exfoliated HGeNSs, and dodecyl-functionalized GeNS prepared using thermally and radical-initiated reactions provides insight into the exfoliation and functionalization processes (Figure 1c). The present HGe-flakes show a Ge−Ge feature at 287 cm^{-1} that is broader than that of the Ge(111) wafer and is shifted to lower energy. These observations are expected because of the incorporation of hydrogen and loss of the long-range structure of crystalline Ge(111). HGe-flakes and exfoliated HGeNSs exhibit comparably broad Ge−Ge features at approximately the same Raman shift (i.e., 289 cm^{-1}). We attribute this observation to the HGeNSs reassembling upon drying during sample preparation. Once functionalization is performed (regardless of the method), reassembly of the GeNSs is not readily possible. The combination of the introduction of dodecyl groups to the GeNS surfaces and the corresponding loss of the underlying structural support of the HGe-flake assembly is reasonably expected to introduce tensile strain into the bonding network of the individual GeNSs; this results in further broadening of the Ge−Ge optical phonon. Similar observations (i.e., Raman shift broadening) have been noted for MoS_2 and WS_2 systems.[37]

The introduction of functionalization-induced tensile strain in the GeNS structure is further made evident by a shift in the optical band gap determined using diffuse reflectance spectroscopy (DRS; Figure S5). We note that the band gap narrows moving from HGeNS (1.7 eV) to radical prepared dodecyl-GeNSs (1.5 eV) to thermally prepared dodecyl-GeNS (1.1 eV). Previous reports of GeNSs suggest longer bonded alkyl surface groups induce greater tensile strain leading to band gap narrowing.[3,30] This is consistent with our observations (*vide infra*, AFM, XPS, TGA) that GeNSs functionalized via radical-initiated reactions bear molecular monolayers while those modified using thermal methods possess surface-bonded oligomers.

Survey XP spectra (Figures S4 and S6) were measured for $CaGe_2$, HGe-flakes, and functionalized GeNSs prepared by both hydrogermylation methods. High-resolution XP spectra of $CaGe_2$, HGe-flakes, as well as dodecyl-GeNS were compared to those of an intrinsic Ge (111) wafer (Figure S6 and Figure 1b). All spectra were calibrated to adventitious carbon at a binding energy (BE) of 284.8 eV.[38] A negatively charged Ge layer stabilized by Ca ions in $CaGe_2$ is made evident by a Ge $3d_{5/2}$ BE of 28.4 eV that appears at lower energy than the Ge emission for the Ge (111) standard (i.e., 29.4 eV). In addition, features associated with surface oxidation of $CaGe_2$ were noted (e.g., O—C═O, 288.5 eV; C—O, 286.0 eV from $CaCO_3$) (Figure S6).[39] The BE of the Ge $3d_{5/2}$ feature in the spectrum of dodecyl-GeNSs prepared using radical-initiated reactions appears at 29.7 eV; this feature appears at similar energy to that observed for HGe-flakes (29.8 eV) and slightly higher energy than that of the Ge standard (29.4 eV). We attribute this shift to the influence of hydrogen and carbon that are bonded to the GeNS surfaces. There are also high-energy shoulders on the Ge spectral features of the dodecyl-GeNSs that we have fit to Ge^{2+} (31.2 eV) and Ge^{4+} (32.4 eV) and attribute to GeOx arising from trace oxidation.[17,36]

Atomic force microscopy (AFM) shows the thicknesses of the sheets prepared using radical-initiated hydrogermylation to be 4.5 nm (Figure 2); this is comparable to surface modified silicane NSs[23,27] and substantially thicker (i.e., ∼8×) than hydride-terminated GeNSs reported elsewhere.[7]

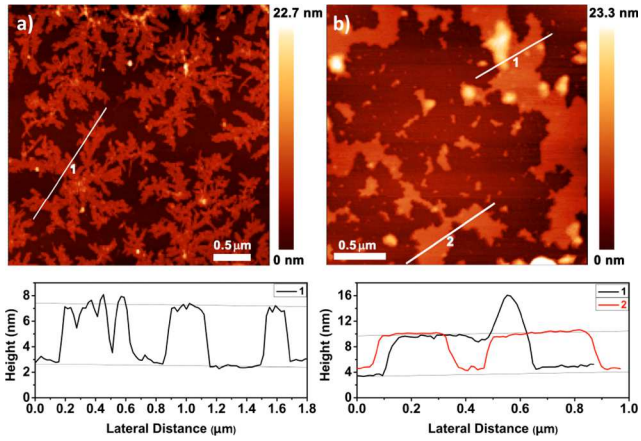

Figure 2. AFM imaging (top) and height profiles (bottom) of dodecyl-terminated GeNSs deposited on clean silicon (111) substrates obtained using (a) radical-initiated and (b) thermally induced methods.

Selected area electron diffraction (SAED) patterns obtained from dodecyl-GeNSs modified via radical-initiated hydrogermylation (Figure 3a) are readily indexed to a simple hexagonal unit cell with a = 3.98 Å with calculated d-spacings of 0.344 and 0.198 nm for the [10$\bar{1}$0] and [11$\bar{2}$0] planes, respectively, assuming a [0001] zone axis. These data are

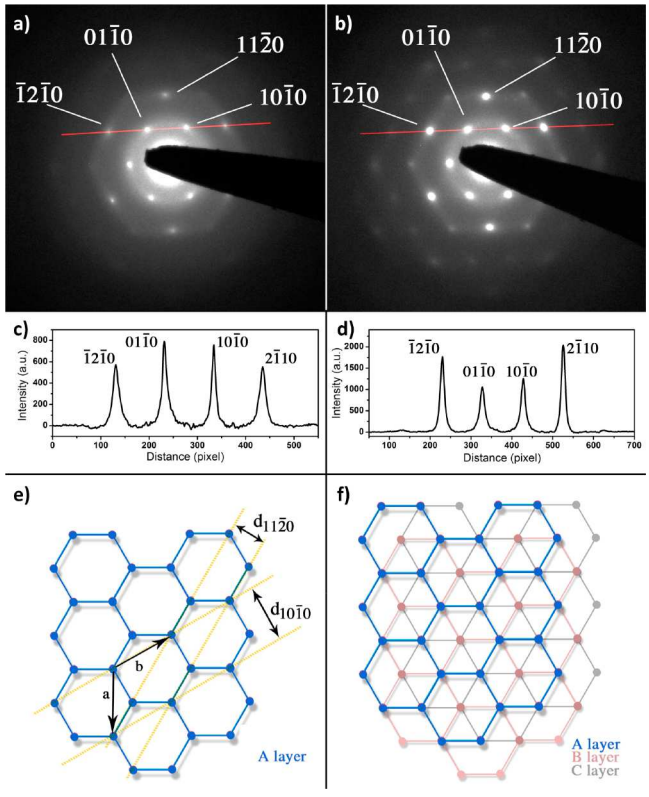

Figure 3. (a, b) Selected electron diffraction patterns of AIBN-functionalized GeNSs along [0001] zone. (c, d) Line profile. (e, f) Corresponding models. Fully (left) and partially (right) exfoliated nanosheets.

DOI: 10.1021/acs.chemmater.7b04974
Chem. Mater. XXXX, XXX, XXX−XXX

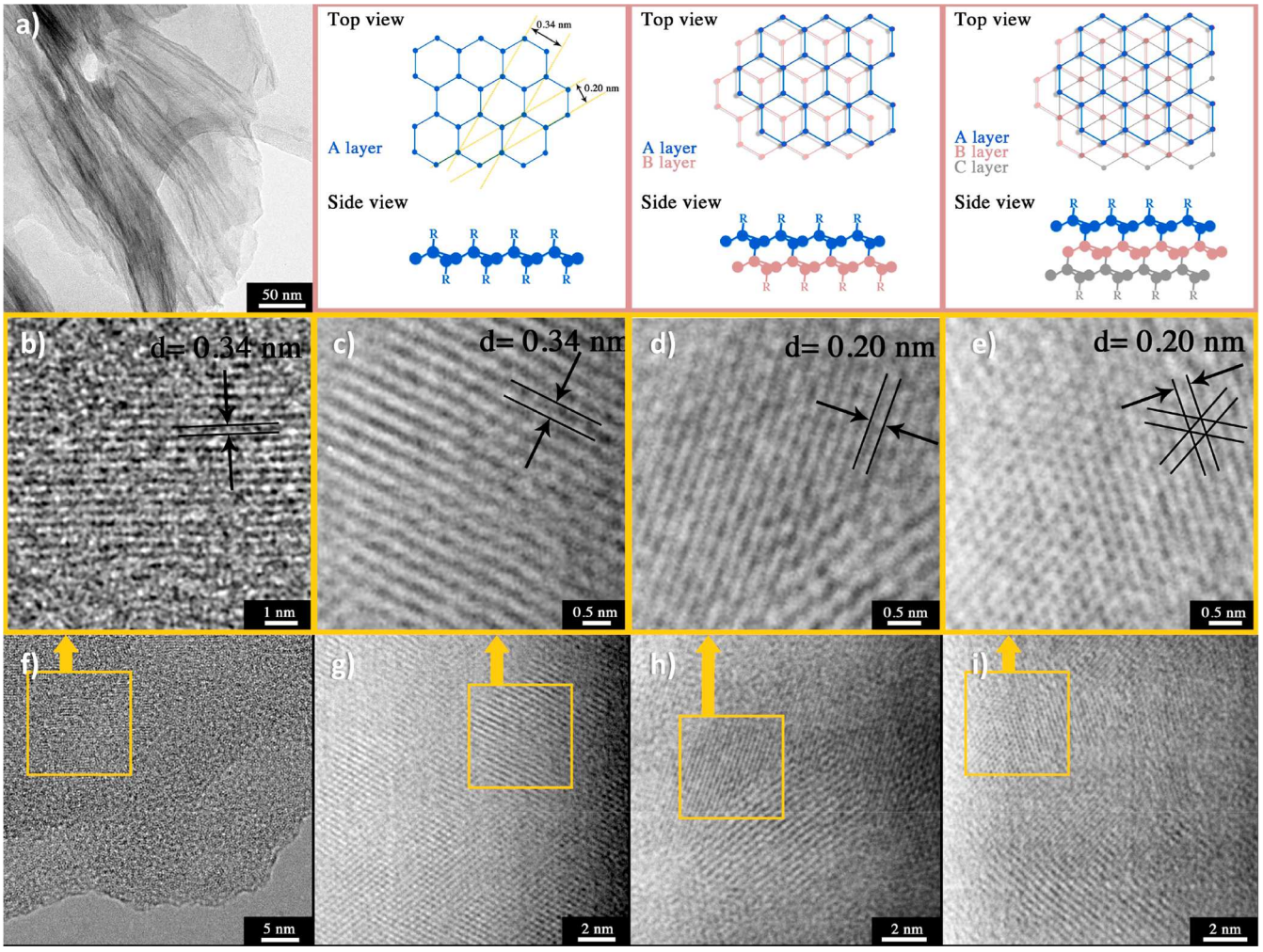

Figure 4. Top: (a) Bright-field TEM and models for Ge nanosheet stacking. Middle: (b–e) Magnified regions of the HRTEM images, shown in (f–i), respectively. Bottom: HRTEM images of thermally modified dodecyl-terminated GeNSs measured at different locations: (f) edge of GeNSs; (g) center of GeNSs; (h, j) partially stacked GeNSs.

consistent with reports of hydride- and methyl-terminated nanosheets.[27] We also note a stronger diffraction intensity for the inner [10$\bar{1}$0] plane when compared to that of the outer [11$\bar{2}$0] plane (see Figure 3a,c); this observation differs from the prediction of the dynamic simulated electron diffraction for AB- and ABC-type germanane stacking (Figure S8) performed using available h2 or tr6 germanane cell parameters, respectively.[40] However, the experimental diffraction intensities we observe mirror those of mechanically exfoliated germanane monolayers[7] as well as graphene structures (e.g., graphene, fluorographene).[41,42]

In contrast, a line profile analysis of the SAED of partially exfoliated GeNSs (i.e., multilayer structures) prepared using radical-initiated hydrogermylation (Figure 3b,d) show a diffraction intensity profile that is in good agreement with simulated AB stacking; of important note, while we can conclude these assemblies are not monolayers, we cannot discount the possibility of these multilayer structures being a mixture of AB and ABC stacking.

Bright-field transmission electron microscopy (TEM) imaging of the present dodecyl-terminated GeNSs indicates they are randomly shaped thin sheets (Figure S9). For GeNSs prepared via thermally induced functionalization, lattice fringes were measured directly using high-resolution TEM (Figure 4). It is important to note that the long-chain alkyl groups on the GeNS surfaces can occlude high-resolution imaging and lead to blurring of lattice fringes; this is not the case for graphene where no pendant surface groups are present. Consistent with the present SAED data (*vide supra*) for dodecyl-terminated GeNSs prepared using radical-induced reactions, the HRTEM analyses afforded lattice spacings of 0.34 nm for [10$\bar{1}$0] planes when evaluating the edges of the GeNS assemblies showing distinct contrast compared to the surrounding vacuum (Figure 4f). Further supporting the conclusion that freestanding GeNSs were prepared using the present methods, we note incremental increases in thickness contrast in TEM imaging (Figure S9) and the same lattice structure away from NS edges (Figure 4g). Unfortunately, direct imaging of the lattice fringes in some stacks is not possible. Presumably visualization is precluded by the presence of long alkyl chains that separate the layers by ≈6 nm (AFM analysis, *vide supra*).

In some cases, we observe lattice fringes for the thermally modified NSs that do not correspond to the [10$\bar{1}$0] spacing (Figure 4d,e). Evaluation of these regions shows a *d*-spacing of 0.20 nm that can correspond to the [11$\bar{2}$0] plane of isolated and/or stacked nanosheets (Figure 4); this is similar to what has previously been reported for graphene.[43]

DOI: 10.1021/acs.chemmater.7b04974
Chem. Mater. XXXX, XXX, XXX–XXX

It is difficult to separate the contributions of isolated and stacked nanosheets to this observation, and multilayers cannot be discounted. However, SAED modeling and data (*vide supra*) indicate detection of the [11$\bar{2}$0] reflection is more likely in multilayer assemblies. In addition, we expect that, for cases where NS stacking is observed, visualization of lattice planes in the HRTEM suggests there is limited separation between Ge layers. We propose that, in these isolated regions, the GeNSs have linked together through Ge−Ge bonds arising from dehydrocoupling reactions. This proposal is further supported by reports of dehydrogenation reactions taking place at elevated temperatures (190 °C).[7] This reactivity is the subject of ongoing studies.

The C 1s and Ge 3d regions of the high-resolution XP spectra of the present dodecyl-GeNSs (Figure S10) were evaluated to estimate the fractional dodecyl monolayer coverage resulting from hydrogermylation reactions. We have applied a ligand−sheet−ligand model of the functionalized GeNS in which both sides (top and bottom) are functionalized (Figure 5a). For these structures, photoelectrons generated

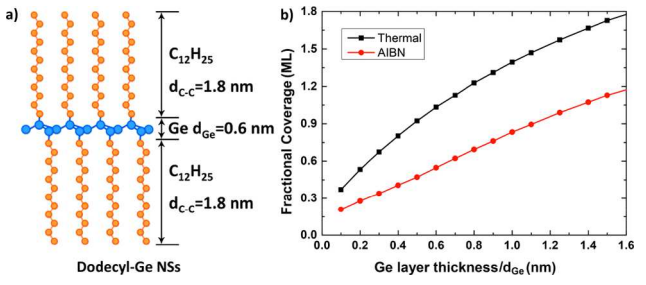

Figure 5. (a) Ideal model for dodecyl-terminated GeNSs (n = 1). (b) Calculated fractional monolayer (ML) ligand coverage determined using eq 1 for indicated Ge layer thicknesses d_{Ge} using XPS, for dodecyl-terminated GeNSs prepared from thermal (black) and AIBN radical (red) hydrogermylation.

from the dodecyl ligands bonded to both NS surfaces and the GeNS itself can be used to estimate the fractional coverage. This approach relies on the following assumptions: (1) The dodecyl-GeNSs are deposited uniformly on the XPS substrate. (2) Carbon appearing in the XP spectrum arises only from the dodecyl functionalities (i.e., there is negligible adventitious carbon), and all emission intensity at 284.8 eV arises from surface tethered dodecyl ligands. (3) The number of edge-bonded ligands is negligible. (4) Each Ge atom is bonded to three other Ge atoms and one alkyl chain (i.e., same atomic volume density). The thickness of the dodecyl ligands bonded to the GeNSs can be estimated using the following equation (derivation presented in Supporting Information; eq 1):

$$\left(\frac{I_{C-C}}{I_{Ge}}\right)\left(\frac{SF_{Ge}}{SF_{C-C}}\right)=\frac{\left(1-e^{-\frac{d_{C-C}}{\lambda_{C-C}}}\right)\left(\sum_{m=1}^{n}e^{-\frac{(2m-1)\cdot d_{C-C}}{\lambda_{C-C}}}+\sum_{m=0}^{n-1}e^{-\frac{2m\cdot d_{C-C}+m\cdot d_{Ge}}{\lambda_{C-C}}}\right)}{\left(1-e^{-\frac{d_{Ge}}{\lambda_{Ge}}}\right)\left(\sum_{m=0}^{n-1}e^{-\frac{(2m+1)\cdot d_{C-C}+m\cdot d_{Ge}}{\lambda_{Ge}}}\right)} \quad (1)$$

where I_{C-C} and I_{Ge} are the integrated intensities of the photoemission peaks from surface tethered alkyl functionalities and GeNSs, respectively; SF_{C-C} and SF_{Ge} are the instrument sensitivity factors for the C 1s (0.278) and Ge 3d (0.536) photoemission signals, respectively; d_{C-C} and d_{Ge} are the thicknesses of the ligand and Ge layers, respectively;[44] and λ_{C-C} and λ_{Ge} are the attenuation lengths of C 1s (3.6 nm) and Ge 3d (2.9 nm) photoelectrons,[45] respectively. The thickness of the dodecyl-terminated GeNSs was determined to be 4.4 nm using tapping mode AFM; in this context, the majority (>99%) of the photoelectrons detected originated from the top three GeNS layers (n = 3).

We performed a series of iterative calculations using eq S6. For these calculations the number of dodecyl-GeNS (n) was defined to n = 10 to ensure that the maximum photoemission intensity was considered. The relationship between monolayer coverage, obtained by dividing d_{C-C} by the fully extended chain length of 1-dodecane (1.8 nm), and d_{Ge} was plotted (Figure 5b).[46] The thickness of each Ge layer was defined as 0.6 nm. Based upon this model, the ligand coverage on dodecyl-GeNSs prepared via radical-initiated reactions was determined to be 0.55 ML (at d_{Ge} = 0.6 nm). This is in excellent agreement with accepted literature values (i.e., 0.5 ML) for the substitution limit for long-chain alkyl groups on flat Ge/Si (111) surfaces,[47−50] and lower than that for Ge nanoparticles (0.62 ML) for which surface curvature is expected to play a role.[19] For dodecyl-GeNSs functionalized using thermally induced hydrogermylation reactions, the coverage (1.03 ML) was found to be more than double the accepted limit on flat Ge (111). This is comparable with observations for thermally induced hydrosilylation on Si (111) surfaces.[49,51−54] Alkyl chain propagation has also been reported for silyl radicals in the case of thermal hydrosilylation on Si NP surface.[32] AFM analysis of these GeNSs sheets shows they are substantially thicker than NSs modified using radical-initiated reactions. These observations suggest the thermally modified dodecyl-GeNSs may be covered by oligomers. The oligomerization of unsaturated ligands can result in even higher surface coverage on curved Ge nanoparticle surfaces when conditions similar to those described here are employed.[21]

The thermal stability of dodecyl-GeNS was investigated using thermogravimetric analysis (TGA). Evaluation of HGeNSs (Figure 6) shows two mass loss events that have previously been attributed to dehydrogenation at 190 °C and chlorine loss starting from 300 to 350 °C.[7] In contrast, dodecyl-GeNSs show no detectable mass loss associated with hydrogen release—this is consistent with the presented surface functionalization. The loss of the dodecyl functionalities resulting from cleavage of Ge−C surface bonds on GeNSs begins spans the 365 to 470 °C and at 475 °C for samples prepared via radical- and thermally activated hydrogermylation, respectively. While the origin of the different thermal responses of the dodecyl-GeNSs is the subject of ongoing investigation, it is reasonably attributed to differences in their surface chemistry noted in the AFM and XPS analyses outlined above.

In conclusion, radical-initiated and thermally induced hydrogermylation reactions were employed to modify hydride-terminated GeNSs. Both hydrogermylation reactions are rapid and afford surface modification. Radical-initiated reactions provide monolayer coverage while thermally activated processes lead to surface oligomerization. As a result, functionalized nanosheets exhibited thicknesses of ∼4.5−5.5 nm depending upon the functionalization method employed. In all cases the Ge atoms are arranged in a buckled simple hexagonal unit cell. In addition, the band gap of the GeNS decreases with surface functionalization and the surface group chain length (i.e., surface group oligomerization). Finally, the thermal stability of functionalized GeNS was increased to 470 °C, which is expected to facilitate ready processing (e.g., blending and extrusion) with functional polymers.

DOI: 10.1021/acs.chemmater.7b04974
Chem. Mater. XXXX, XXX, XXX−XXX

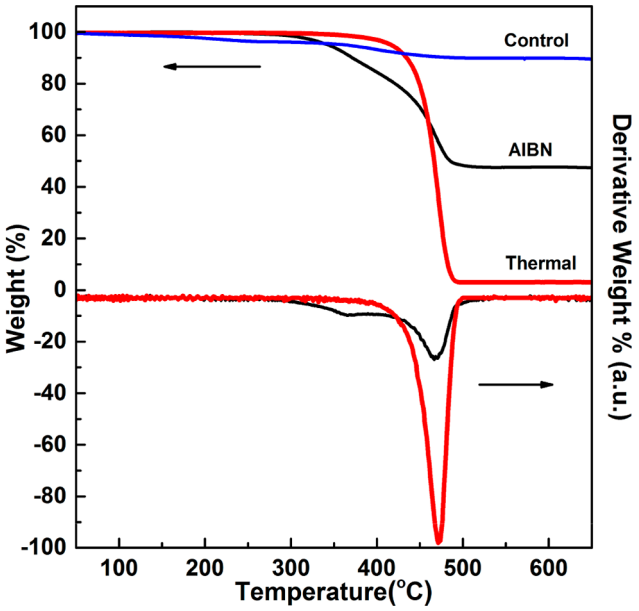

Figure 6. Thermogravimetric analysis (TGA; top, left axis) and derivative thermogravimetric (DTG; bottom, right axis) of GeNSs functionalized through AIBN (black) and thermally induced (red) methods, respectively. The TGA profile of H-terminated GeNS is provided for comparison (blue).

■ ASSOCIATED CONTENT

Supporting Information

The Supporting Information is available free of charge on the ACS Publications website at DOI: 10.1021/acs.chemmater.7b04974.

Additional data including functionalization methods, surface calculation procedure, pXRD pattern of precursors, XPS survey and high-resolution spectra, DRS of precursor and functionalized GeNSs, SAED simulation pattern, and bright-field TEM images (PDF)

■ AUTHOR INFORMATION

Corresponding Author

*E-mail: jveinot@ualberta.ca.

ORCID

Haoyang Yu: 0000-0002-0748-9414

Bernhard Rieger: 0000-0002-0023-884X

Jonathan G.C. Veinot: 0000-0001-7511-510X

Notes

The authors declare no competing financial interest.

■ ACKNOWLEDGMENTS

The authors recognize continued generous funding from the Natural Sciences and Engineering Research Council of Canada (NSERC Discovery Grant program) as well as NSERC CREATE and Deutsche Forschungsgemeinschaft DFG (IRTG2022) for Alberta/Technical University of Munich International Graduate School for Hybrid Functional Materials (ATUMS). We also thank the staff at Analytical and Instrumentation Laboratory in the Department of Chemistry at the University of Alberta for the assistance with FTIR and TGA analysis, Drs. Shihong Xu and Anqiang He of the UofA NanoFab for their assistance with XPS, and Dr. Morteza Javadi for assistance with Raman spectroscopy. T.H. gratefully acknowledges funding from Studienstiftung des deutschen Volkes. Thanks are also conveyed to all Veinot Team members for useful discussions.

■ REFERENCES

(1) Geim, A. K.; Grigorieva, I. V. Van Der Waals Heterostructures. *Nature* **2013**, *499*, 419−425.

(2) Okamoto, H.; Sugiyama, Y.; Nakano, H. Synthesis and Modification of Silicon Nanosheets and Other Silicon Nanomaterials. *Chem. - Eur. J.* **2011**, *17*, 9864−9887.

(3) Nicolosi, V.; Chhowalla, M.; Kanatzidis, M. G.; Strano, M. S.; Coleman, J. N. Liquid Exfoliation of Layered Materials. *Science* **2013**, *340*, 1226419.

(4) Lopez-Sanchez, O.; Lembke, D.; Kayci, M.; Radenovic, A.; Kis, A. Ultrasensitive Photodetectors Based on Monolayer MoS_2. *Nat. Nanotechnol.* **2013**, *8*, 497−501.

(5) Geim, A. K. Graphene: Status and Prospects. *Science* **2009**, *324*, 1530−1534.

(6) Lee, C.; Wei, X.; Kysar, J. W.; Hone, J. Measurement of the Elastic Properties and Intrinsic Strength of Monolayer Graphene. *Science* **2008**, *321*, 385−388.

(7) Bianco, E.; Butler, S.; Jiang, S.; Restrepo, O. D.; Windl, W.; Goldberger, J. E. Stability and Exfoliation of Germanane: A Germanium Graphane Analogue. *ACS Nano* **2013**, *7*, 4414−4421.

(8) Li, L.; Lu, S.; Pan, J.; Qin, Z.; Wang, Y.; Wang, Y.; Cao, G.; Du, S.; Gao, H.-J. Buckled Germanene Formation on Pt(111). *Adv. Mater.* **2014**, *26*, 4820−4824.

(9) Dávila, M. E.; Xian, L.; Cahangirov, S.; Rubio, A.; Lay, G. L. Germanene: A Novel Two-Dimensional Germanium Allotrope Akin to Graphene and Silicene. *New J. Phys.* **2014**, *16*, 095002.

(10) Vogt, P.; De Padova, P.; Quaresima, C.; Avila, J.; Frantzeskakis, E.; Asensio, M. C.; Resta, A.; Ealet, B.; Le Lay, G. Silicene: Compelling Experimental Evidence for Graphenelike Two-Dimensional Silicon. *Phys. Rev. Lett.* **2012**, *108*, 155501.

(11) Tao, L.; Cinquanta, E.; Chiappe, D.; Grazianetti, C.; Fanciulli, M.; Dubey, M.; Molle, A.; Akinwande, D. Silicene Field-Effect Transistors Operating at Room Temperature. *Nat. Nanotechnol.* **2015**, *10*, 227−231.

(12) Wöhler, F. Ueber Verbindungen Des Siliciums Mit Sauerstoff Und Wasserstoff. *Justus Liebigs Ann. Chem.* **1863**, *127*, 257−274.

(13) Vogg, G.; Brandt, M. S.; Stutzmann, M.; Genchev, I.; Bergmaier, A.; Görgens, L.; Dollinger, G. Epitaxial $CaGe_2$ Films on Germanium. *J. Cryst. Growth* **2000**, *212*, 148−154.

(14) Vogg, G.; Brandt, M. S.; Stutzmann, M. Polygermyne—A Prototype System for Layered Germanium Polymers. *Adv. Mater.* **2000**, *12*, 1278−1281.

(15) Balendhran, S.; Walia, S.; Nili, H.; Sriram, S.; Bhaskaran, M. Elemental Analogues of Graphene: Silicene, Germanene, Stanene, and Phosphorene. *Small* **2015**, *11*, 640−652.

(16) Cahangirov, S.; Topsakal, M.; Aktürk, E.; Şahin, H.; Ciraci, S. Two- and One-Dimensional Honeycomb Structures of Silicon and Germanium. *Phys. Rev. Lett.* **2009**, *102*, 236804.

(17) Prabhakaran, K.; Ogino, T. Oxidation of Ge(100) and Ge(111) Surfaces: An UPS and XPS Study. *Surf. Sci.* **1995**, *325*, 263−271.

(18) Bodlaki, D.; Yamamoto, H.; Waldeck, D. H.; Borguet, E. Ambient Stability of Chemically Passivated Germanium Interfaces. *Surf. Sci.* **2003**, *543*, 63−74.

(19) Buriak, J. M. Organometallic Chemistry on Silicon and Germanium Surfaces. *Chem. Rev.* **2002**, *102*, 1271−1308.

(20) Choi, K.; Buriak, J. M. Hydrogermylation of Alkenes and Alkynes on Hydride-Terminated Ge(100) Surfaces. *Langmuir* **2000**, *16*, 7737−7741.

(21) Javadi, M.; Picard, D.; Sinelnikov, R.; Narreto, M. A.; Hegmann, F. A.; Veinot, J. G. C. Synthesis and Surface Functionalization of Hydride-Terminated Ge Nanocrystals Obtained from the Thermal Treatment of $Ge(OH)_2$. *Langmuir* **2017**, *33*, 8757−8765.

(22) Helbich, T.; Lyuleeva, A.; Ludwig, T.; Scherf, L. M.; Fässler, T. F.; Lugli, P.; Rieger, B. One-Step Synthesis of Photoluminescent

DOI: 10.1021/acs.chemmater.7b04974
Chem. Mater. XXXX, XXX, XXX−XXX

Covalent Polymeric Nanocomposites from 2D Silicon Nanosheets. *Adv. Funct. Mater.* **2016**, *26*, 6711−6718.
(23) Helbich, T.; Lyuleeva, A.; Höhlein, I. M. D.; Marx, P.; Scherf, L. M.; Kehrle, J.; Fässler, T. F.; Lugli, P.; Rieger, B. Radical-Induced Hydrosilylation Reactions for the Functionalization of Two-Dimensional Hydride Terminated Silicon Nanosheets. *Chem. - Eur. J.* **2016**, *22*, 6194−6198.
(24) Okamoto, H.; Kumai, Y.; Sugiyama, Y.; Mitsuoka, T.; Nakanishi, K.; Ohta, T.; Nozaki, H.; Yamaguchi, S.; Shirai, S.; Nakano, H. Silicon Nanosheets and Their Self-Assembled Regular Stacking Structure. *J. Am. Chem. Soc.* **2010**, *132*, 2710−2718.
(25) Okamoto, H.; Sugiyama, Y.; Nakanishi, K.; Ohta, T.; Mitsuoka, T.; Nakano, H. Surface Modification of Layered Polysilane with N-Alkylamines, α,ω-Diaminoalkanes, and ω-Aminocarboxylic Acids. *Chem. Mater.* **2015**, *27*, 1292−1298.
(26) Sugiyama, Y.; Okamoto, H.; Mitsuoka, T.; Morikawa, T.; Nakanishi, K.; Ohta, T.; Nakano, H. Synthesis and Optical Properties of Monolayer Organosilicon Nanosheets. *J. Am. Chem. Soc.* **2010**, *132*, 5946−5947.
(27) Nakano, H.; Nakano, M.; Nakanishi, K.; Tanaka, D.; Sugiyama, Y.; Ikuno, T.; Okamoto, H.; Ohta, T. Preparation of Alkyl-Modified Silicon Nanosheets by Hydrosilylation of Layered Polysilane (Si_6H_6). *J. Am. Chem. Soc.* **2012**, *134*, 5452−5455.
(28) Jiang, S.; Arguilla, M. Q.; Cultrara, N. D.; Goldberger, J. E. Improved Topotactic Reactions for Maximizing Organic Coverage of Methyl Germanane. *Chem. Mater.* **2016**, *28*, 4735−4740.
(29) Jiang, S.; Butler, S.; Bianco, E.; Restrepo, O. D.; Windl, W.; Goldberger, J. E. Improving the Stability and Optical Properties of Germanane via One-Step Covalent Methyl-Termination. *Nat. Commun.* **2014**, *5*, 3389.
(30) Jiang, S.; Krymowski, K.; Asel, T.; Arguilla, M. Q.; Cultrara, N. D.; Yanchenko, E.; Yang, X.; Brillson, L. J.; Windl, W.; Goldberger, J. E. Tailoring the Electronic Structure of Covalently Functionalized Germanane via the Interplay of Ligand Strain and Electronegativity. *Chem. Mater.* **2016**, *28*, 8071−8077.
(31) Purkait, T. K.; Iqbal, M.; Wahl, M. H.; Gottschling, K.; Gonzalez, C. M.; Islam, M. A.; Veinot, J. G. C. Borane-Catalyzed Room-Temperature Hydrosilylation of Alkenes/Alkynes on Silicon Nanocrystal Surfaces. *J. Am. Chem. Soc.* **2014**, *136*, 17914−17917.
(32) Yang, Z.; Iqbal, M.; Dobbie, A. R.; Veinot, J. G. C. Surface-Induced Alkene Oligomerization: Does Thermal Hydrosilylation Really Lead to Monolayer Protected Silicon Nanocrystals? *J. Am. Chem. Soc.* **2013**, *135*, 17595−17601.
(33) Höhlein, I. M. D.; Werz, P. D. L.; Veinot, J. G. C.; Rieger, B. Photoluminescent Silicon Nanocrystal-Polymer Hybrid Materials via Surface Initiated Reversible Addition−fragmentation Chain Transfer (RAFT) Polymerization. *Nanoscale* **2015**, *7*, 7811−7818.
(34) Grimme, S. Semiempirical GGA-Type Density Functional Constructed with a Long-Range Dispersion Correction. *J. Comput. Chem.* **2006**, *27*, 1787−1799.
(35) Paton, K. R.; Varrla, E.; Backes, C.; Smith, R. J.; Khan, U.; O'Neill, A.; Boland, C.; Lotya, M.; Istrate, O. M.; King, P.; et al. Scalable Production of Large Quantities of Defect-Free Few-Layer Graphene by Shear Exfoliation in Liquids. *Nat. Mater.* **2014**, *13*, 624−630.
(36) Holmberg, V. C.; Korgel, B. A. Corrosion Resistance of Thiol- and Alkene-Passivated Germanium Nanowires. *Chem. Mater.* **2010**, *22*, 3698−3703.
(37) Ramakrishna Matte, H. S. S.; Gomathi, A.; Manna, A. K.; Late, D. J.; Datta, R.; Pati, S. K.; Rao, C. N. R. MoS_2 and WS_2 Analogues of Graphene. *Angew. Chem., Int. Ed.* **2010**, *49*, 4059−4062.
(38) Miller, D. J.; Biesinger, M. C.; McIntyre, N. S. Interactions of CO2 and CO at Fractional Atmosphere Pressures with Iron and Iron Oxide Surfaces: One Possible Mechanism for Surface Contamination? *Surf. Interface Anal.* **2002**, *33*, 299−305.
(39) Boehm, H. P. Surface Oxides on Carbon and Their Analysis: A Critical Assessment. *Carbon* **2002**, *40*, 145−149.
(40) Cultrara, N. D.; Wang, Y.; Arguilla, M. Q.; Scudder, M. R.; Jiang, S.; Windl, W.; Bobev, S.; Goldberger, J. E. Synthesis of 1T, 2H, and 6R Germanane Polytypes. *Chem. Mater.* **2018**, *30*, 1335−1343.
(41) Hernandez, Y.; Nicolosi, V.; Lotya, M.; Blighe, F. M.; Sun, Z.; De, S.; McGovern, I. T.; Holland, B.; Byrne, M.; Gun'Ko, Y. K.; et al. High-Yield Production of Graphene by Liquid-Phase Exfoliation of Graphite. *Nat. Nanotechnol.* **2008**, *3*, 563−568.
(42) Meyer, J. C.; Geim, A. K.; Katsnelson, M. I.; Novoselov, K. S.; Obergfell, D.; Roth, S.; Girit, C.; Zettl, A. On the Roughness of Single- and Bi-Layer Graphene Membranes. *Solid State Commun.* **2007**, *143*, 101−109.
(43) Horiuchi, S.; Gotou, T.; Fujiwara, M.; Sotoaka, R.; Hirata, M.; Kimoto, K.; Asaka, T.; Yokosawa, T.; Matsui, Y.; Watanabe, K.; et al. Carbon Nanofilm with a New Structure and Property. *Jpn. J. Appl. Phys.* **2003**, *42*, L1073−L1076.
(44) Plymale, N. T.; Dasog, M.; Brunschwig, B. S.; Lewis, N. S. A Mechanistic Study of the Oxidative Reaction of Hydrogen-Terminated Si(111) Surfaces with Liquid Methanol. *J. Phys. Chem. C* **2017**, *121*, 4270−4282.
(45) Szajman, J.; Jenkin, J. G.; Liesegang, J.; Leckey, R. C. G. Electron Mean Free Paths in Ge in the Range 70−1400 EV. *J. Electron Spectrosc. Relat. Phenom.* **1978**, *14*, 41−48.
(46) Kim, D.; Joo, J.; Pan, Y.; Boarino, A.; Jun, Y. W.; Ahn, K. H.; Arkles, B.; Sailor, M. J. Thermally Induced Silane Dehydrocoupling on Silicon Nanostructures. *Angew. Chem., Int. Ed.* **2016**, *55*, 6423−6427.
(47) Wallart, X.; Henry de Villeneuve, C.; Allongue, P. Truly Quantitative XPS Characterization of Organic Monolayers on Silicon: Study of Alkyl and Alkoxy Monolayers on H−Si(111). *J. Am. Chem. Soc.* **2005**, *127*, 7871−7878.
(48) Sieval, A. B.; van den Hout, B.; Zuilhof, H.; Sudhölter, E. J. R. Molecular Modeling of Covalently Attached Alkyl Monolayers on the Hydrogen-Terminated Si(111) Surface. *Langmuir* **2001**, *17*, 2172−2181.
(49) Knapp, D.; Brunschwig, B. S.; Lewis, N. S. Chemical, Electronic, and Electrical Properties of Alkylated Ge(111) Surfaces. *J. Phys. Chem. C* **2010**, *114*, 12300−12307.
(50) Cullen, G. W.; Amick, J. A.; Gerlich, D. The Stabilization of Germanium Surfaces by Ethylation I. Chemical Treatment. *J. Electrochem. Soc.* **1962**, *109*, 124−127.
(51) Loscutoff, P. W.; Bent, S. F. REACTIVITY OF THE GERMANIUM SURFACE: Chemical Passivation and Functionalization. *Annu. Rev. Phys. Chem.* **2006**, *57*, 467−495.
(52) Chen, R.; Bent, S. F. Highly Stable Monolayer Resists for Atomic Layer Deposition on Germanium and Silicon. *Chem. Mater.* **2006**, *18*, 3733−3741.
(53) Sharp, I. D.; Schoell, S. J.; Hoeb, M.; Brandt, M. S.; Stutzmann, M. Electronic Properties of Self-Assembled Alkyl Monolayers on Ge Surfaces. *Appl. Phys. Lett.* **2008**, *92*, 223306.
(54) Webb, L. J.; Nemanick, E. J.; Biteen, J. S.; Knapp, D. W.; Michalak, D. J.; Traub, M. C.; Chan, A. S. Y.; Brunschwig, B. S.; Lewis, N. S. High-Resolution X-Ray Photoelectron Spectroscopic Studies of Alkylated Silicon(111) Surfaces. *J. Phys. Chem. B* **2005**, *109*, 3930−3937.

DOI: 10.1021/acs.chemmater.7b04974
Chem. Mater. XXXX, XXX, XXX−XXX